

Adsorption, desorption, and clustering of H₂O on Pt(111)

John L. Daschbach, Brandon M. Peden, R. Scott Smith, and Bruce D. Kay

Citation: *The Journal of Chemical Physics* **120**, 1516 (2004); doi: 10.1063/1.1633752

View online: <http://dx.doi.org/10.1063/1.1633752>

View Table of Contents: <http://scitation.aip.org/content/aip/journal/jcp/120/3?ver=pdfcov>

Published by the [AIP Publishing](#)

Articles you may be interested in

[Kinetic study of the “surface explosion” phenomenon in the N O + C O reaction on Pt\(100\) through dynamic Monte Carlo simulation](#)

J. Chem. Phys. **128**, 134705 (2008); 10.1063/1.2885048

[Low coverage spontaneous etching and hyperthermal desorption of aluminum chlorides from Cl₂ / Al \(111\)](#)

J. Chem. Phys. **121**, 9018 (2004); 10.1063/1.1805495

[A helium atom scattering study of the adsorption of NO on Pt\(111\)](#)

J. Chem. Phys. **112**, 7600 (2000); 10.1063/1.481354

[Collision induced desorption and dissociation of O₂ on Pt\(111\)](#)

J. Chem. Phys. **109**, 737 (1998); 10.1063/1.476612

[Dynamics of collision-induced desorption: Ar–Xe/Pt\(111\)](#)

J. Chem. Phys. **106**, 3370 (1997); 10.1063/1.473086



Launching in 2016!
The future of applied photonics research is here

AIP | APL
Photonics

Adsorption, desorption, and clustering of H₂O on Pt(111)

John L. Daschbach, Brandon M. Peden, R. Scott Smith, and Bruce D. Kay^{a)}
*Chemical Sciences Division, Fundamental Science Directorate, Pacific Northwest National Laboratory,
 Mail Stop K8-88, Richland, Washington 99352*

(Received 10 September 2003; accepted 22 October 2003)

The adsorption, desorption, and clustering behavior of H₂O on Pt(111) has been investigated by specular He scattering. The data show that water adsorbed on a clean Pt(111) surface undergoes a structural transition from a random distribution to clustered islands near 60 K. The initial helium scattering cross sections as a function of temperature are found to be insensitive to the incident H₂O flux over a range of 0.005 monolayers (ML)/s–0.55 ML/s indicating that the clustering process is more complex than simple surface diffusion. The coarsening process of an initially random distribution of water deposited at 25 K is found to occur over a broad temperature range, 60 < *T* < 140 K, during thermal annealing. The desorption kinetics for submonolayer water are determined to be zero order for surface coverages greater than 0.05 ML and temperatures between 145 and 172 K. The zero-order desorption kinetics are consistent with a two-dimensional two-phase coexistence between a high-density H₂O condensed phase (islands) and a low-density two-dimensional gaslike phase on the Pt surface. © 2004 American Institute of Physics. [DOI: 10.1063/1.1633752]

I. INTRODUCTION

The interaction of water with well-defined metal surfaces continues to be of considerable interest due to the central importance of these two materials in surface physics and the general importance of water/surface interactions in nature.^{1,2} The structure of water for submonolayer coverages θ has been investigated on a number of close-packed transition-metal surfaces by a range of techniques. These include infrared absorption spectroscopy on Pt(111),^{3,4} electron energy-loss spectroscopy on Pt(111),⁵ low-energy electron diffraction (LEED),⁶ He atom scattering on Pt(111)^{7–9} and Rh(111),¹⁰ scanning tunneling microscopy (STM) studies on Pt(111)^{11,12} and on Pd(111),¹³ and numerous others listed in Appendix A of a recent review article by Henderson.²

Under appropriate growth conditions a single layer of water is thought to form a hexagonal honeycomb structure on Pt(111). This has long been considered a structure with alternating oxygen atoms in each sixfold ring of water molecules staggered normal to the surface plane with the lower three considered to be bonded to the metal via the lone pair on the oxygen.^{1,2,6,7} This is the so-called “bilayer” structure that has been reported for H₂O on other metals^{1,2} and for which there is a detailed discussion for H₂O on Ru(001).¹⁴ However, a more recent low-energy electron diffraction (LEED) study of H₂O on Ru(001) suggests that all of the O atoms are nearly co-planar.¹⁵ A combined x-ray and computational study by Ogasawara *et al.*¹⁶ also contradicts the bilayer picture and predicts that the first water layer is flat on Pt(111) when the multilayer is annealed at 140 K. Recent density-functional theory (DFT) calculations propose that the near coplanar geometry could be explained by a half-dissociated water layer.^{17–19} However, a recent study of the

structure of D₂O on Ru(001) using sum frequency generation vibrational spectroscopy finds that the adsorbed D₂O remains intact.²⁰ They propose a bilayer structure where every other water molecule exhibits a hydrogen-metal substrate bond.²⁰ Clearly, the monolayer structure of water on metals is still an active and contentious area of research.

Atomic resolution STM studies of H₂O on Ag(111),²¹ Pd(111),¹³ and Pt(111)^{11,12} can provide a great deal of information on the structure of submonolayer water. In the Pd(111)/H₂O system at temperatures between 40 and 55 K the diffusion and clustering of water molecules has been imaged with time resolved methods and the diffusion coefficient of monomers, dimers, trimers, and tetramers determined.¹³ These larger cluster units diffuse faster than the monomers and the proposed mechanism for this increased diffusion is a combination of increased hydrogen bonding between the water molecules and a lattice mismatch with the substrate. A distribution of cluster sizes and shapes is reported with increasing water coverage, eventually growing into stable hexagonal rings and ultimately into an ordered honeycomb overlayer with ($\sqrt{3} \times \sqrt{3}$) R30°.

Morgenstern *et al.* have studied the behavior of H₂O on Pt(111) between 135 and 148 K with STM and determined the adsorption sites and adsorbate structures.^{11,12} They conclude that the most stable site for H₂O adsorption is the upper side of steps on the Pt(111) surface where quasi-one-dimensional (1D) chains are formed.¹¹ At higher coverages, two-dimensional ice islands grow out from the lower side of step edges. Upon raising the temperature of a sample with a complete bilayer to 145 K, vacancy islands are formed by desorption of some H₂O molecules. These vacancy islands are mobile on the time scale of the STM scanning, indicating that substantial detachment and reattachment takes place on the edges on the H₂O islands. In further work¹² they determine that at 140 K there are three 2D solid phases of different densities and a 2D liquid phase which is determined to be

^{a)}Author to whom correspondence should be addressed. Fax: (509) 376-6066. Electronic mail: Bruce.Kay@pnl.gov

more dense than any of the solid phases. The solid phases may be transformed into each other by suitable application of temperature and H₂O pressure but require the presence of the liquid phase. Partial melting of the 2D solid phases is observed between 130 and 148 K but coexistence of 2D solid and liquid phases is observed over this entire temperature range.

Additional evidence for the melting of the bilayer phase comes from infrared vibrational spectroscopy.⁴ The infrared spectrum for submonolayer D₂O adsorbed at 25 K was assigned to monomers and dimers. Changes in the spectrum upon heating were attributed to conversion of the system to a structured bilayer phase. It was proposed that at 85 K gaslike monomers on the surface were in equilibrium with the bilayer ice structure. Further heating of the system between 105 and 125 K led to changes which were assigned to the coexistence of a liquidlike phase with the bilayer structure. Heating to 155 K resulted in the disappearance of spectral features assigned to bilayer ice and the water was considered a liquid phase. Quenching of the 155 K system did not restore the bilayer structure and the system was now regarded as amorphous solid water (ASW).

High-resolution He atom scattering has been used to investigate the vibrational dynamics and adsorption characteristics of submonolayer water on Pt(111).⁸ Three structural regimes were assigned at low coverage, for $T < 40$ K the primary water entities are monomers, for $T > 40$ K stable dimers and trimers were found, while for $T > 100$ –130 K large two-dimensional bilayer islands formed.

There have been a number of reports of submonolayer water desorption kinetics for Pt(111) using temperature programmed desorption (TPD).^{6,22–24} The earlier work generally described the single monolayer peak as having near or pseudo zero-order kinetics²² but later work found two peaks and interpreted them as first order.²⁴ The two peaks were ascribed to desorption from bilayer ice at 170 K and nonbilayer regions at 177 K and the relative intensities were dependent on deposition temperature with higher temperatures leading to an increased desorption rate for the bilayer feature. More recent high quality TPD spectra finds only the single monolayer peak and interprets this as fractional order kinetics between zero and first order.⁶ Ogasawara *et al.*⁴ also reported observing only one peak in the monolayer region.

The structure of a full bilayer of water grown on Pt(111) at 137 K has been determined by LEED (Ref. 6) to be $(\sqrt{39} \times \sqrt{39}) R16.2^\circ$. No LEED pattern was resolved below completion of the bilayer. At this temperature the bilayer film acts as a epitaxial template with orientation preserved up to 5 BL. Above this coverage, or when annealed, the film restructures to the $R30^\circ$ bulk ice overlayer.²⁵ He atom scattering has determined the same structure for the complete bilayer and a $(\sqrt{37} \times \sqrt{37}) R25.3^\circ$ structure at sub-bilayer coverage.⁷

While a great deal is known about the structure of water on Pt(111) at submonolayer coverage, the effect of the structure and coverage on the desorption kinetics is unresolved. As well, the clustering upon adsorption and the coarsening of adsorbed water, has been investigated only at broadly or moderately spaced finite temperatures. Here we report He

specular scattering and TPD measurements which address these two issues.

II. EXPERIMENT

The experiments were performed in an ultrahigh vacuum (UHV) chamber with a base pressure below 1×10^{-10} Torr. The sample was a 1 cm diameter Pt(111) disk, 2 mm thick. The sample was spot welded to two tantalum wire leads, 2 mm in diameter, clamped in a gold plated copper jig attached to a closed-cycle He cryostat, and resistively heated through the tantalum leads. The temperature was monitored with a K-type thermocouple and controlled by computer over a range of 20–1300 K. The temperature was calibrated using the adsorption and desorption rates of argon multilayers that were then referenced to tabulated values for the argon vapor pressure.^{26,27} The calibration was checked by comparing the desorption of H₂O ice multilayers with tabulated vapor pressure data²⁶ and previous publications.^{28,29} We estimate the error in the absolute temperature to be less than ± 2 K. The relative isothermal temperature stability was better than 0.05 K. The surface purity and order of the Pt(111) substrate were checked using Auger electron spectroscopy (AES) and low-energy electron diffraction (LEED). Immediately prior to each experiment the sample was flashed to 1000 K and then cooled to the initial experimental temperature. Cooling from 1000 to 20 K required about 250 sec.

The supersonic He beam was produced by expanding the pure gas (Air Liquide, research grade) through a 100 μ m diameter aperture with a backing pressure of 1000 Torr and a nozzle temperature of 300 K. The kinetic energy distribution was estimated to be $E/\Delta E$ (full width at half maximum) > 5 . The quasieffusive H₂O beam was produced by expanding the gas between 0.1 and 2.0 Torr through a 1 mm diameter aperture. The data reported here were taken with the He and H₂O beams at 45° and 30° with respect to the sample normal. Both beams were quadruply-differentially pumped prior to impinging on the Pt(111) target. Electronically controlled shutters between the second and third differential pumping stages allowed for control of the water fluence to better than 0.01 monolayer (ML). The H₂O beam is about 8 mm diameter on the sample at normal incidence and the He beam is about 5 mm diameter centered within the H₂O spot. The He flux was about $10^{15} \text{ cm}^{-2} \text{ s}^{-1}$ and the H₂O flux was varied between 10^{13} and $10^{15} \text{ cm}^{-2} \text{ s}^{-1}$. For the water coverage, we define 1 ML as the saturation coverage of a H₂O monolayer determined using temperature programmed desorption and we estimate the error in the coverage to be $\pm 5\%$. The He specular signal was monitored with a quadrupole mass spectrometer equipped with an integrating cup with a 3 mm aperture in the scattering plane 3 cm from the sample. The detector angular resolution, measured by rotating the mass spectrometer about the sample, was about 15°.

Thermal energy atom scattering (TEAS), or specular He scattering, is a sensitive probe of adsorbate structure on close-packed metal surfaces.³⁰ A clean Pt(111) surface is nearly mirrorlike for a He beam with the relative intensity of the first-order diffracted beam $< 10^{-3}$. Temperature effects are accounted for by plotting the specularly scattered He intensity I relative to that from a clean surface I_0 at that same

temperature. The sensitivity of the TEAS technique is due to the relatively large scattering cross sections observed for many adsorbates at low coverages. For example, the scattering cross section Σ for isolated CO molecules at low coverage is about 125 \AA^2 .³¹ In contrast, the area occupied by a typical densely packed adsorbate ($\theta \approx 1$, 10^{15} cm^{-2}) is about 10 \AA^2 . The difference is because He atoms are scattered out of the specular direction by interaction with the attractive part of the molecular potential, and as a result, isolated molecules can have large scattering cross sections. As the adsorbate surface density increases or as adsorbates cluster, the individual scattering cross sections overlap and the overall apparent scattering cross section decreases. The coverage dependence of the relative scattering intensity thus depends on the adsorbate structure. Three possible cases for the two-dimensional adsorbate structure are fully random, random on lattice sites, and fully clustered into islands. For these cases, the relative specular He intensity as a function of coverage is given by³⁰

$$\frac{I}{I_0} = \exp(-\theta n_s \Sigma), \quad (1)$$

$$\frac{I}{I_0} = (1 - \theta)^{n_s \Sigma}, \quad (2)$$

$$\frac{I}{I_0} = 1 - \theta n_s A, \quad (3)$$

respectively, where θ is the relative coverage, n_s is the number density of the adsorption sites, Σ is the scattering cross section in the low coverage limit, and A is the surface area of a closely packed adsorbate molecule (islands). The coverage dependence of the relative scattering intensity I/I_0 shown in Eqs. (1)–(3) is then used to infer information about the adsorbate structure.

III. RESULTS

A. H₂O clustering kinetics

Figure 1 displays a set of isothermal He scattering measurements for a series of Pt(111) substrate temperatures. The relative helium scattering I/I_0 is plotted as a function of exposure time to a 0.057 ML/s H₂O beam. As discussed above, the relevant quantity is the dependence of the relative helium scattering on adsorbate surface coverage. The coverage and exposure time are related by the condensation coefficient which is dependent on several parameters including the sticking coefficient, incident flux, substrate temperature, and desorption kinetics.³² For all of the data shown here, except the 156 K experiment, the condensation coefficient was constant and close to 1 (>0.95) and thus a direct calculation of the coverage was possible. The upper x axis is the corresponding coverage calculated assuming an H₂O condensation coefficient of 1.

The specular helium scattering signal for all of the temperatures shown decreases with increasing H₂O coverage, with, however, different coverage dependences. In the 27 K experiment, I/I_0 decreases exponentially with H₂O coverage. As the substrate temperature is increased, the I/I_0 wave

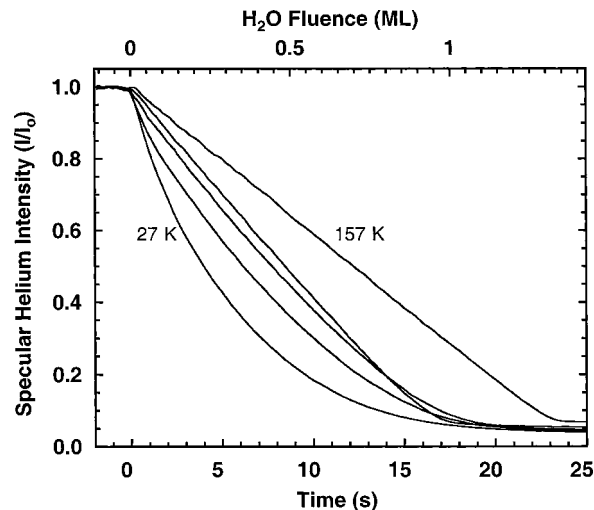


FIG. 1. The relative specular He intensity I/I_0 versus time for a Pt(111) substrate exposed to a 0.057-ML/s flux H₂O beam. The time axis is relative to the initiation of the H₂O beam and I_0 is the specular intensity from an initially clean substrate. The results are for a series of isothermal experiments where the substrate temperature was 27, 67, 92, 122, and 157 K. The upper x axis is the corresponding H₂O coverage calculated using a condensation coefficient of 1. The condensation coefficient is one (>0.95) for all the experiments displayed here except for the 156 K experiment.

forms become more linear with the 122 and 157 K data being nearly linear over the entire coverage range. The exponential coverage dependence observed at low temperature is consistent with Eq. (1) which predicts an adsorbate structure of randomly distributed isolated water molecules. On the other hand, the linear coverage dependence observed at higher temperature is consistent with Eq. (3) which predicts an adsorbate structure where the water has clustered into two-dimensional islands. The data in Fig. 1 suggest that there is a transition in the H₂O structure from randomly distributed isolated molecules at low temperatures to clustered islands at higher temperatures.

The above temperature-dependent structural transition should also be apparent in the initial scattering cross sections. Figure 2 is a plot of the initial scattering cross section as a function of substrate temperature. The initial cross section is the slope obtained from a linear fit to the first 10% of the I/I_0 versus coverage (time) curve. At substrate temperatures less than 60 K the scattering cross section is relatively large and nearly constant. Between 60 and 75 K there is a significant decrease in the cross section. Above 80 K the cross section shows a very gradual decrease. These data support the structural transition proposed above. That is, at low temperatures the cross section is relatively large because there is very little water clustering, and thus there is very little overlap in the scattering potential. At higher temperatures, the apparent cross section is reduced due to the overlap of the scattering potentials of the clustered water. The data in Fig. 2 suggest that this transition occurs between 60 and 75 K. This is consistent with the temperature range where the onset of H₂O surface mobility is observed on Pd(111).¹³

The initial cross-section data in Fig. 2 differ from those reported by Glebov *et al.*⁸ who report a cross section of 130 \AA^2 at 23 K whereas our value is about 30 \AA^2 . They also

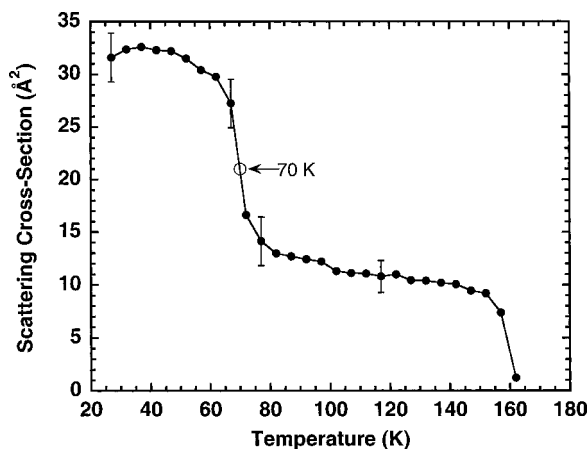


FIG. 2. The apparent initial He scattering cross sections as a function of substrate temperature. The H₂O flux was 0.22 ML/s. The apparent initial cross section was extracted from the first 10% decrease in the specular helium intensity I/I_0 after initiation of H₂O beam. The open circle at 70 K is shown as a temperature reference. Representative error bars are shown on a few data points.

observe a strong temperature dependence between 23 and 60 K. These differences are likely due to the larger detector acceptance angle of 15° in our experiment versus the 0.3° used by Glebov *et al.*^{8,9} The large cross sections arise from large impact parameter, small deflection angle scattering by the long-range attractive region of the interaction potential. Because of our large detector acceptance angle we are insensitive to cross sections greater than $\sim 30 \text{ Å}^2$. Despite the quantitative differences in the absolute cross section, the relative changes in the initial cross section with temperature provide clear evidence for a change in the submonolayer structure near 60 K.

The clustering of randomly deposited adsorbates depends on the surface diffusion kinetics of isolated molecules. The length L that a deposited molecule will diffuse in a characteristic time t is related to the diffusion rate D by the equation $L = \sqrt{Dt}$. The characteristic time is defined by the time interval a molecule has to move before being hit and bound by an impinging molecule. Thus, by varying the incident water flux, there should be a shift in the temperature where the clustering transition occurs. The relationship between the incident flux and the clustering temperature can then be used to determine the surface diffusion kinetics. The results of experiments where the flux was varied from 0.005 to 0.55 ML/s were quantitatively identical (within experimental uncertainty) i.e., the results were independent of the incident flux. This is despite an estimate, using recently published surface diffusion parameters for H₂O on Pd(111) ($E_a = 12.3 \text{ kJ/mole}$ and $\nu = 10^{12} \text{ s}^{-1}$),¹³ that predicts that an 8 K shift in the clustering transition should occur over this flux range. The flux independence of the clustering transition temperature suggests that the process is more complex than simple surface diffusion.

The coarsening of an initially random distribution of water was studied to further investigate the above structural transition. Various coverages of H₂O were deposited at 25 K, and the helium scattering was measured as the sample was heated. In principle, as the randomly distributed H₂O mol-

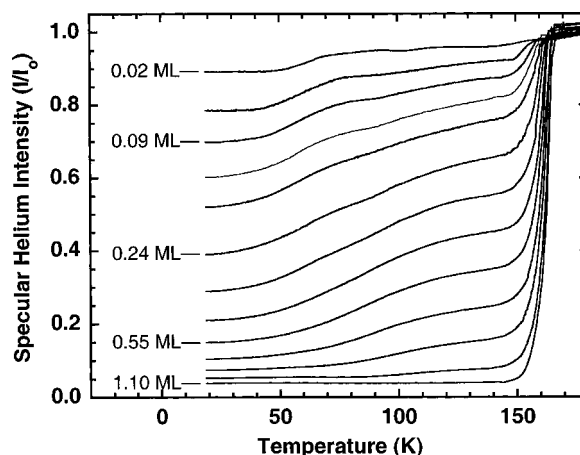


FIG. 3. The specular helium intensity I/I_0 versus substrate temperature for various initial coverages of H₂O deposited at 20 K and a flux 0.22 ML/s. After the H₂O was deposited the temperature was ramped at 4 K/s. From top to bottom the initial coverages are 0.02, 0.05, 0.09, 0.13, 0.18, 0.27, 0.36, 0.45, 0.55, 0.64, 0.73, 0.82, and 1.1 ML.

ecules begin to cluster, the specular He intensity should increase. Figure 3 shows a series of these experiments where the initial coverage of water deposited at 25 K ranged from 0.02 ML to a full monolayer. The helium scattering was then monitored as a 4 K/s temperature ramp was applied. The values for I_0 were obtained from the clean Pt(111) surface over the same temperature range. The difference between I_0 at 20 and 160 K was less than 5%.

The initial value of I/I_0 decreases with increasing coverage, thus the lowest initial coverage curve is at the top (highest initial I/I_0) and the highest initial coverage curve is at the bottom. The 0.02 ML coverage curve (top in Fig. 3), shows a relatively sharp increase in the relative specular intensity, I/I_0 , near $\sim 60 \text{ K}$. An increase in I/I_0 corresponds to a decrease in the nonspecular scattering and thus represents a decrease in the apparent scattering cross section. Subsequent curves with increasing initial coverages show that the transition in the I/I_0 shifts to higher temperature and occurs over a wider temperature range. The highest coverage curve, $\theta \approx 1$, shows no change in I/I_0 with temperature, which is the expected behavior for a completed monolayer. Above about 150 K all of the curves show a large increase in the specular intensity due to H₂O desorption. Above 155 K where the helium scattering should be from clean Pt(111), there is a range of specular intensities close to 1. Because this deviation from 1 is larger for smaller initial coverages, we think that the deviation is due to the adsorption of small amounts of background impurities (CO, H₂) during the experiment.

The data in Fig. 3 show that there is wide range of temperatures where the initially random dilute water molecules cluster. The lack of a clear clustering transition temperature again supports the observation that the clustering kinetics are complex.

Thermal vibrations in both the substrate and the adsorbates can attenuate the scattering intensity and this is the so-called Debye-Waller effect.³³ We do not think that the changes we observe in the relative helium scattering with temperature are due to Debye-Waller effects. First the

Debye–Waller effects would cause a decrease in the specular intensity with temperature whereas we observe an increase in the specular helium intensity. Second, if we stop the ramp at a given temperature and cool the sample back to 20 K there is minimal change in the specular helium intensity. Thus the changes in the specular helium intensity are due to structural changes that occur as the sample is heated and not due to Debye–Waller changes in the scattering intensity with temperature. Based on published Debye–Waller factors for water,⁹ one would expect a factor of 20 decrease in the specular intensity between a sample at 20 and 150 K. Again, because of our relatively large detector acceptance angle, we are not affected by Debye–Waller temperature effects and the changes we observe are due primarily to changes in submonolayer water structure. The use of the broad detector acceptance angle both increases the total signal and drastically reduces Debye–Waller effects thereby enabling us to perform the kinetic studies described herein.

The reduction in nonspecular He scattering (an increase in I/I_0 the specular intensity) could arise from two effects. The first would be a reduction in the number density of isolated, or low coordination, H₂O molecules as the temperature is increased. The second would be the Ostwald ripening of the water islands, with larger islands growing and smaller islands disappearing. The latter could explain why in the higher coverage experiments, the changes in the scattering occur over a broad temperature range. This ripening process is too slow to be observed within an experimentally accessible time in isothermal experiments (~ 1000 s due to the background adsorption of contaminants). However, if the sample heating is stopped at a given temperature and cooled the absolute signal changes less than 5%. This suggests that the changes in the submonolayer water structure with temperature are irreversible.

B. H₂O adsorption and desorption kinetics

The time-dependent coverage of an adsorbate on a substrate is simply equal to the difference between the adsorption rate and the desorption rate, $d\theta/dt = J_{\text{ads}}(\theta, T) - J_{\text{des}}(\theta, T)$. The adsorption rate is a product of the incident flux J_{in} and the sticking coefficient $S(\theta, T)$, which, in general, can be coverage and temperature dependent. However, the sticking coefficient for H₂O has previously been shown to be near unity (>0.95) and to be independent of coverage and temperature.³² Therefore in our experiments, J_{ads} is directly equal to J_{in} , and the time-dependent coverage equation simplifies to $d\theta/dt = J_{\text{in}} - J_{\text{des}}(\theta, T)$. From this equation and the time-dependent coverage data one can extract the adsorption and desorption kinetics.

The adsorption and desorption kinetics are revealed in the temporal behavior of the helium scattering. Figure 4 displays the relative specular He reflectivity for a set of isothermal measurements with temperatures ranging from 150 to 160 K. In these experiments, the sample is exposed to a 0.057 ML/s flux H₂O beam for 120 s. At $t = 0$, the start of the exposure, the value of I/I_0 decreases from 1 to near 0 due to the net adsorption of H₂O. In this part of the experiment, $d\theta/dt$ is equal to $J_{\text{in}} - J_{\text{des}}(\theta, T)$. The data show that the

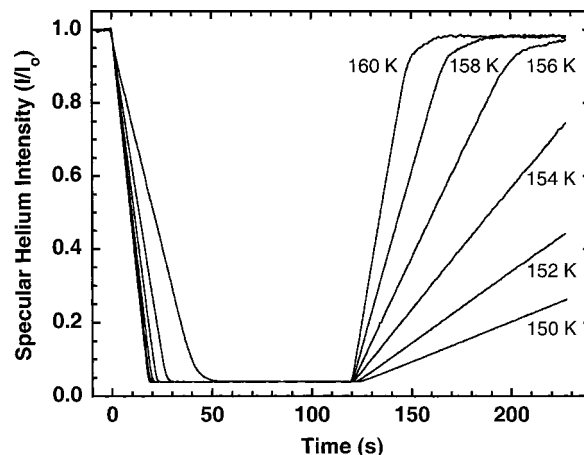


FIG. 4. The specular helium intensity I/I_0 from a Pt(111) substrate held at various isothermal temperatures during and after the transient illumination with a 0.057 ML/s flux H₂O beam. The time axis is relative to the start of a 120 s exposure to the H₂O beam. At $t = 120$ s the beam is turned off. The temperatures shown are 150, 152, 154, 156, 158, and 160 K.

decrease in I/I_0 is linear, albeit with slightly different slopes for each of the curves. The observed linear decrease means that $J_{\text{in}} - J_{\text{des}}(\theta, T)$ is constant and hence $J_{\text{des}}(\theta, T)$ is constant. If $J_{\text{des}}(\theta, T)$ is constant as the coverage increases, then the desorption rate must be coverage independent, i.e., the submonolayer desorption kinetics are zero order. The differences in the slopes of the individual isothermal experiments are due to the temperature dependence of the desorption rate.

Once a monolayer has formed the value of I/I_0 remains constant until the incident water beam is turned off at $t = 120$ s. Upon termination of the H₂O beam, the value of I/I_0 for all of the curves increases linearly from near zero to unity. The curves are linear for almost 95% of the desorption with only a slight deviation from linearity as I/I_0 approaches 1. This deviation is likely due to the desorption of H₂O that is adsorbed at defect sites and hence more strongly bound. At this point in the experiment, since $J_{\text{in}} = 0$, the slope of the individual curves is a direct measure of the isothermal desorption rates. In the adsorption part of the experiment (beam on), the variation in the slopes is less, simply due to the fact that the slope is a measure of the net adsorption rate (i.e., $J_{\text{in}} - J_{\text{des}}$). The linear response of I/I_0 after the beam is turned off again suggests that the submonolayer desorption kinetics are zero order.

The coverage independence of the desorption kinetics can be confirmed by measuring the desorption rate as a function of the initial substrate coverage. A similar approach was used by Wu *et al.* to study the H₂O desorption from Ag(011).³⁴ In our experiments an H₂O beam is exposed to the substrate for varying lengths of time to create a series of initial coverages. The termination time of the H₂O beam defines the initial coverage and after which the desorption rate is determined. Figure 5 displays the relative helium scattering results in which a 0.22 ML/s H₂O beam was used to create various initial coverages on the Pt(111) substrate held at 151 K. The data show that when the H₂O beam is turned on, I/I_0 decreases due to the net adsorption of H₂O. Because the substrate temperature and incident flux are the

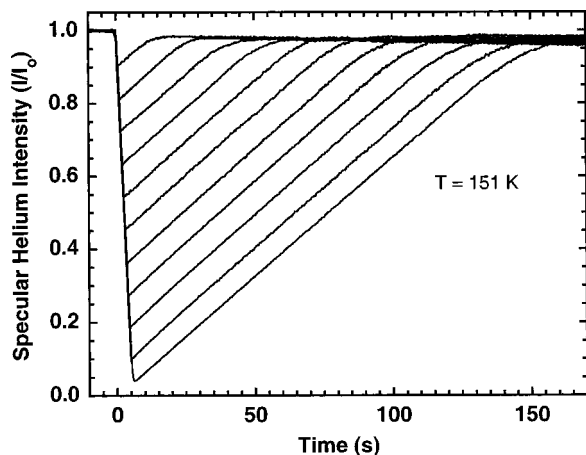


FIG. 5. The specular helium intensity I/I_0 from a Pt(111) substrate held at 151 K during and after the transient illumination with a 0.22 ML/s flux H₂O beam for varying exposure times to create a series of initial coverages. At $t=0$, the H₂O beam is turned on and I/I_0 decreases due to the net adsorption of H₂O. At various times the H₂O beam is shut off and I/I_0 increases as the coverage decreases due to desorption. The increase in I/I_0 for all of the curves is linear and these linear curves are parallel.

same, the curves lie exactly on top of each other during the adsorption portion of the experiment (beam on). When the H₂O beam is turned off, I/I_0 increases as the coverage decreases due to desorption. The increase in I/I_0 for all of the curves is linear and these linear curves are parallel. The slope of these lines is directly equal to the desorption rate. A constant and equal slope means that the desorption rate is the same regardless of the initial and constantly changing substrate coverage. These results confirm that the desorption kinetics of H₂O from Pt(111) are zero order over a wide range of coverages.

The temperature dependence of the desorption kinetics was studied by conducting isothermal experiments from 150–174 K. In these experiments, a monolayer of H₂O was deposited on the substrate and the helium scattering during the desorption of the H₂O was used to determine the desorption rate. Figure 6 displays a representative set of results from 150 to 160 K in 2 K steps. In the figure, the relative helium scattering intensity has been converted to the corresponding coverage and plotted versus time. The data show that for all temperatures, the decrease in coverage with time is linear from 1 to <0.1 ML. As mentioned above, the curvature below 0.1 ML is likely the result of the much slower desorption rate of water adsorbed on defects. A linear decrease in coverage with time is the signature of zero-order kinetics and the slope of this linear decrease is the isothermal desorption rate. An Arrhenius plot of the desorption rates for 247 isothermal experiments spanning the temperature range 145–172 K is shown in Fig. 7. An Arrhenius fit to the data (solid line) gave kinetic parameters of $\nu = 1.4 \pm 3.5 \times 10^{16}$ ML/s and $E_a = 54.2 \pm 3$ kJ/mole. This activation energy compares well with the 52 ± 2 -kJ/mole value reported by Haq *et al.*⁶

The desorption rate parameters from the isothermal helium scattering measurements above were compared to the results obtained by temperature programmed desorption (TPD). Figure 8 shows a series of TPD spectra for a range of

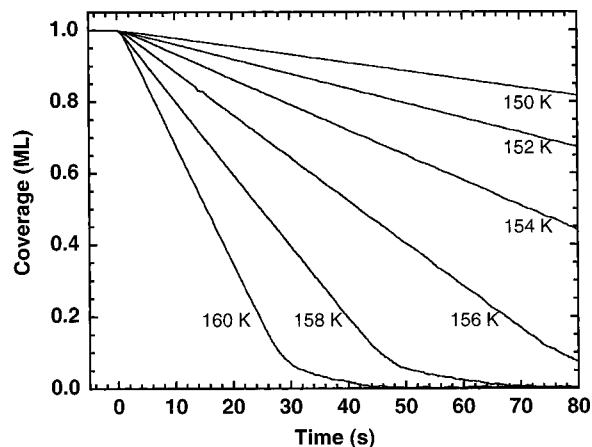


FIG. 6. The coverage versus time obtained from isothermal He scattering transients after a monolayer of H₂O has been adsorbed and the incident beam turned off. Substrate temperatures are 150–160 K in 2 K increments. A linear decrease in coverage with time is the signature of zero-order kinetics and the slope of this linear decrease is the isothermal desorption rate.

H₂O coverages from 0.1 to 1.0 ML taken at a linear ramp rate of 0.6 K/s. The coalescence of the leading edges of the submonolayer TPD spectra is a characteristic of zero-order desorption kinetics. The dashed line is the desorption rate calculated using the Arrhenius parameters obtained in Fig. 7. The calculated rate and the leading edges of the TPD spectra are in excellent agreement.

IV. DISCUSSION AND SUMMARY

The results clearly show that the submonolayer H₂O structure on Pt(111) is strongly dependent on the substrate temperature during adsorption. The temperature dependence of both the relative helium scattering with coverage (Fig. 1) and the initial scattering cross-section data (Fig. 2) support this conclusion. The data suggest that the structural transition from randomly isolated H₂O molecules to clustered islands occurs around 60 K. This observation is consistent with pre-

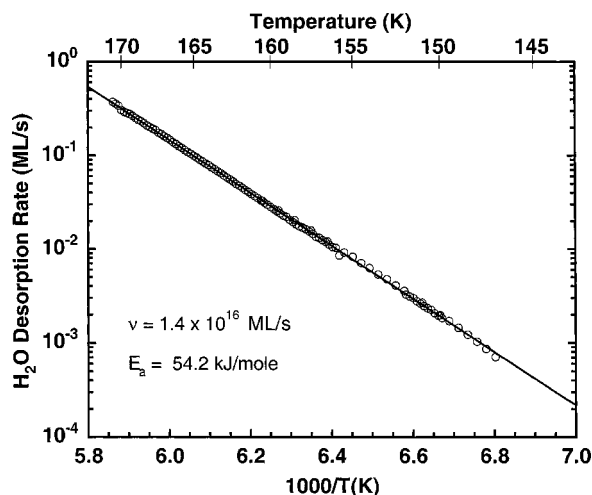


FIG. 7. An Arrhenius plot of the desorption rates for 247 independent isothermal experiments spanning the temperature range 145–172 K. The solid line is a fit to the data with the kinetic parameters of $\nu = 1.4 \times 10^{16} \pm 0.4$ ML/s and $E_a = 54.2 \pm 3$ kJ/mole.

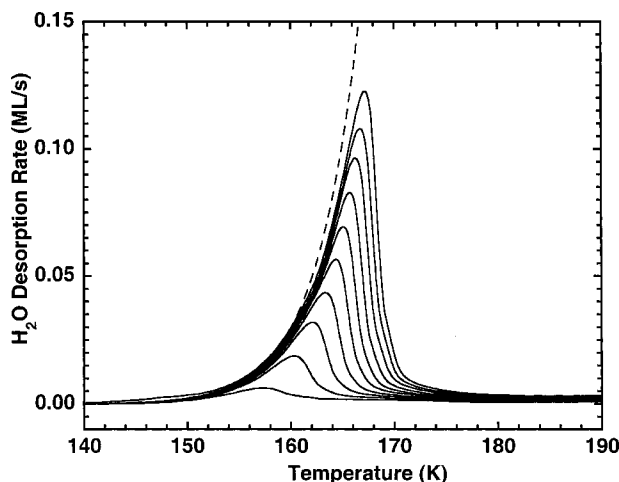


FIG. 8. Temperature programmed desorption of H_2O from Pt(111). The H_2O was deposited at 100 K with a flux of 0.22 ML/s and then heated at a rate of 0.6 K/s. The initial coverages of water 0.1, 0.2, 0.3, 0.4, 0.5, 0.6, 0.7, 0.8, 0.9, and 1.0 ML. The dashed line is calculated from the Arrhenius parameters obtained in Fig. 7.

vious investigations by STM,¹² vibrational spectroscopy,^{4,6} He scattering,⁸ and LEED,⁶ where water on Pt(111) has been shown to go from isolated molecules through a sequence of higher coordination species, to a dense 2D condensed phase. However, the flux independence of the clustering transition temperature that we observe suggests that the clustering mechanism is more complex than simple surface diffusion. This is further supported by our observation of the broadening of the clustering transition temperature with coverage as an initially random distribution of H_2O molecules clusters upon heating (Fig. 3). A possible explanation for the complexity could be the co-existence of multiple phases on the surface. This has been observed previously on Pt(111) for rare gases using helium scattering³¹ and for submonolayer H_2O using STM.^{11,12} Furthermore, the morphology of the clustered water is highly dynamic due to processes such as Ostwald ripening whereby large clusters grow as small clusters decay.¹³

The results in Figs. 4–7 clearly show that the submonolayer desorption kinetics of H_2O from Pt(111) are zero order over a wide range of coverages (0.1–1 ML) and temperatures (150–170 K). The desorption rates obtained from the isothermal helium scattering measurements are in excellent agreement with TPD measurements (Fig. 8). Near zero-order kinetics have been reported previously for the water Pt(111) system^{6,22} and interpreted in terms of individual mechanistic steps, or using a dynamical description of the desorption process.³⁵ Similarly, zero-order desorption has been reported for the water Ag(011) surface³⁴ and interpreted with a detailed mean-field treatment of the desorption mechanism. Here we make use of a thermodynamic argument to explain the submonolayer zero-order desorption kinetics. At temperatures lower than we can measure desorption, 145 K, STM results¹¹ show that the two-dimensional islands become fuzzy and this is interpreted as the onset of melting. If desorption were only from the surface or edges of the two-dimensional islands then complex compensating kinetics

would be required for zero-order desorption to occur over the coverage ($0.1 < \theta < 1.0$) and temperature in the ($150 < T < 174$ K) range observed here. If however, we assume that the two-dimensional condensed phase is in equilibrium with a two-dimensional gaslike phase, then by detailed balance with unity sticking and far from a phase boundary, the desorption rate is a direct measure of the vapor pressure.^{28,36,37} Application of the phase rule leaves only one degree of freedom in the system, the chemical potential μ , and therefore the vapor pressure over the system is determined uniquely by the temperature. Such behavior has been seen for many systems and for adsorbates with attractive interactions. Simple lattice gas models give rise to wide ranges of isothermal coverage independent chemical potential.³³ Water desorption from Pt(111), over the coverage and temperature range studied here, is strictly zero order, and is a consequence of a two-dimensional, two-phase coexistence between a gas phase and a condensed phase.

As discussed by Kevan and co-workers³⁴ and Kreuzer and Payne,³⁵ a quasiequilibrium in the adsorbate layer will be maintained if the rate of desorption into the three-dimensional gas phase is slow relative to the kinetic processes involved in establishing the two-dimensional equilibrium. For systems where the sticking coefficient is unity and coverage independent, and the adsorbate interactions are attractive, a two-dimensional, two-phase coexistence should exist, and as such, the desorption kinetics will be zero order even in the submonolayer regime.

One may ask if it is surprising that water desorption exhibits zero-order kinetics over the coverage range $0.1 \leq \theta < 1$ and in the temperature range $145 \leq T < 172$ K. Based on the two phase thermodynamic equilibrium argument presented above, zero-order kinetics will be observed if a two-phase coexistence exists over this coverage and temperature range. To address this question, it is instructive to consider the range of “average” densities for which condensed phase three-dimensional water (liquid or solid) coexists with a three-dimensional vapor. At 300 K, the number density of liquid water is $3.34 \times 10^{22} \text{ cm}^{-3}$ and the equilibrium vapor pressure is $3.57 \times 10^3 \text{ Pa}$ (~ 27 Torr) which corresponds to a molecular number density of $8.6 \times 10^{17} \text{ cm}^{-3}$. At 160 K, the density of crystalline ice is $3.08 \times 10^{22} \text{ cm}^{-3}$ and the equilibrium vapor pressure is $1.33 \times 10^{-4} \text{ Pa}$ ($\sim 1 \times 10^{-6}$ Torr) which corresponds to a density of $6.0 \times 10^{10} \text{ cm}^{-3}$. At a given temperature, the density of the two-phase system can range from that of the condensed phase (essentially all water is condensed) to the density of the vapor (nearly all water exists as vapor). Hence the two-phase liquid (ice)/vapor coexistence of three-dimensional water spans an “average” density range ($\Delta \rho_{3D} = \rho_{\text{condensed}} / \rho_{\text{vapor}}$) of factors of 3.85×10^4 and 5.13×10^{11} at 300 and 160 K, respectively.

Heuristically, we expect that the same attractive interactions responsible for the two-phase coexistence of three-dimensional water will give rise to the coexistence of two-dimensional high-density condensed and low-density gaslike phases in water adsorbed on Pt(111). To account for the reduced dimensionality of the two-dimensional adsorbate system, we rescale the three-dimensional density range using

the relation $\Delta\rho_{2D} \sim (\Delta\rho_{3D})^{2/3}$. Rescaling the 160 K three-dimensional data ($\Delta\rho_{3D} = 5.13 \times 10^{11}$) results in a two-dimensional two-phase coexistence over a density range of a factor of 6.5×10^7 ! As evident from this simple calculation, we expect that near 160 K water adsorbed on Pt(111) should display two-phase coexistence over a coverage range spanning roughly eight orders of magnitude. Clearly the presence of morphological defects (steps, kinks, etc.) on the Pt(111) substrate will dominate the kinetics at low coverages. Nonetheless, the simple calculation presented above demonstrates that zero-order desorption kinetics for H₂O adsorbed on Pt(111) are expected over essentially the entire coverage range as is observed experimentally.

ACKNOWLEDGMENTS

We wish to acknowledge Glenn Teeter and Zdenek Donahalek for helpful scientific discussions and Derek Hopkins for instrumental software development. This work was supported by the U. S. Department of Energy, Office of Basic Energy Sciences, Chemical Sciences Division. Pacific Northwest National Laboratory is operated for the U. S. Department of Energy by Battelle under Contract No. DE-AC06-76RLO 1830.

¹P. A. Thiel and T. E. Madey, *Surf. Sci. Rep.* **7**, 211 (1987).

²M. A. Henderson, *Surf. Sci. Rep.* **46**, 5 (2002).

³H. Ogasawara, J. Yoshinobu, and M. Kawai, *Chem. Phys. Lett.* **231**, 188 (1994).

⁴H. Ogasawara, J. Yoshinobu, and M. Kawai, *J. Chem. Phys.* **111**, 7003 (1999).

⁵K. Jacobi, K. Bedurftig, Y. Wang, and G. Ertl, *Surf. Sci.* **472**, 9 (2001).

⁶S. Haq, J. Harnett, and A. Hodgson, *Surf. Sci.* **505**, 171 (2002).

⁷A. Glebov, A. P. Graham, A. Menzel, and J. P. Toennies, *J. Chem. Phys.* **106**, 9382 (1997).

⁸A. L. Glebov, A. P. Graham, and A. Menzel, *Surf. Sci.* **428**, 22 (1999).

⁹A. Glebov, A. P. Graham, A. Menzel, J. P. Toennies, and P. Senet, *J. Chem. Phys.* **112**, 11011 (2000).

¹⁰K. D. Gibson, M. Viste, and S. J. Sibener, *J. Chem. Phys.* **112**, 9582 (2000).

¹¹M. Morgenstern, T. Michely, and G. Comsa, *Phys. Rev. Lett.* **77**, 703 (1996).

¹²M. Morgenstern, J. Muller, T. Michely, and G. Comsa, *Z. Phys. Chem. (Munich)* **198**, 43 (1997).

¹³T. Mitsui, M. K. Rose, E. Fomin, D. F. Ogletree, and M. Salmeron, *Science* **297**, 1850 (2002).

¹⁴D. L. Doering and T. E. Madey, *Surf. Sci.* **123**, 305 (1982).

¹⁵G. Held and D. Menzel, *Surf. Sci.* **316**, 92 (1994).

¹⁶H. Ogasawara, B. Brena, D. Nordlund, M. Nyberg, A. Pelmenchikov, L. G. M. Pettersson, and A. Nilsson, *Phys. Rev. Lett.* **89**, 276102 (2002).

¹⁷P. J. Feibelman, *Science* **295**, 99 (2002).

¹⁸P. J. Feibelman, *Phys. Rev. B* **67**, 035420 (2003).

¹⁹A. Michaelides, A. Alavi, and D. A. King, *J. Am. Chem. Soc.* **125**, 2746 (2003).

²⁰D. N. Denzler, C. Hess, R. Dudek, S. Wagner, C. Frischkorn, M. Wolf, and G. Ertl, *Chem. Phys. Lett.* **376**, 618 (2003).

²¹K. Morgenstern, *Surf. Sci.* **504**, 293 (2002).

²²G. B. Fisher and J. L. Gland, *Surf. Sci.* **94**, 446 (1980).

²³H. Ibach and S. Lehwald, *Surf. Sci.* **91**, 187 (1980).

²⁴S. K. Jo, J. Kiss, J. A. Polanco, and J. M. White, *Surf. Sci.* **253**, 233 (1991).

²⁵U. Starke, N. Materer, A. Barbieri, R. Doll, K. Heinz, M. A. Vanhove, and G. A. Somorjai, *Surf. Sci.* **287**, 432 (1993).

²⁶R. E. Honig and H. O. Hook, *RCA Rev.* **21**, 360 (1960).

²⁷H. Schlichting and D. Menzel, *Rev. Sci. Instrum.* **64**, 2013 (1993).

²⁸R. J. Speedy, P. G. Debenedetti, R. S. Smith, C. Huang, and B. D. Kay, *J. Chem. Phys.* **105**, 240 (1996).

²⁹K. P. Stevenson, G. A. Kimmel, Z. Dohnalek, R. S. Smith, and B. D. Kay, *Science* **283**, 1505 (1999).

³⁰G. Comsa and B. Poelsema, in *Atomic and Molecular Beam Methods*, edited by G. Scoles (Oxford University Press, Oxford, 1992), Vol. 2, p. 463.

³¹G. Comsa, K. Kern, and B. Poelsema, in *Helium Atom Scattering from Surfaces*, edited by H. Hulpke (Springer-Verlag, Berlin, 1992), Vol. 27, p. 243.

³²D. E. Brown, S. M. George, C. Huang, E. K. L. Wong, K. B. Rider, R. S. Smith, and B. D. Kay, *J. Phys. Chem.* **100**, 4988 (1996).

³³A. Zangwill, *Physics at Surfaces* (Cambridge University Press, Cambridge, England, 1988).

³⁴K. J. Wu, L. D. Peterson, G. S. Elliott, and S. D. Kevan, *J. Chem. Phys.* **91**, 7964 (1989).

³⁵H. J. Kreuzer and S. H. Payne, in *Equilibria and Dynamics of Gas Adsorption on Heterogeneous Solid Surfaces*, edited by W. Rudzinski, W. A. Steele, and G. Zgrablich (Elsevier, New York, 1997), Vol. 104, p. 153.

³⁶S. D. Kevan, D. C. Skelton, and D. H. Wei, *Crit. Rev. Surf. Chem.* **4**, 77 (1994).

³⁷S. D. Kevan, *J. Mol. Catal. A: Chem.* **131**, 19 (1998).